Anesthetic-Enhanced Membrane Fusion Examined Using Two-Photon Fluorescence Correlation Spectroscopy

Jody L. Swift,[†] Anna Carnini,[†] Tanya E. S. Dahms,[‡] and David T. Cramb*[,†]

Department of Chemistry, 2500 University Drive, N.W., University of Calgary, Calgary, AB, T2N 1N4 Canada, and Department of Chemistry and Biochemistry, University of Regina, Regina, SK, S4S 0A2 Canada

Received: November 26, 2003; In Final Form: March 31, 2004

Vesicle fusion has been used as a model for viral fusion with cells, but measuring the kinetics of the process simultaneously with vesicle size has been elusive. In this study, we describe the use of two-photon excitation fluorescence cross-correlation spectroscopy (TPE-XCS) to measure simultaneously the kinetics and structural changes occurring early in the process of vesicle fusion. We have shown that in the presence of a novel fusion agent, halothane, unilamellar vesicles of dioleoylphosphatidylcholine fuse at rates slower than the diffusion limit. We postulate that halothane works as a gentle perturbation agent by increasing the disorder in the phospholipid bilayer. Moreover, under the conditions used in the present study, this process appears to be complete when approximately six vesicles have fused.

Introduction

Membrane fusion is crucial to the proper functioning of eukaryotic cells. This process facilitates merging one subcellular compartment with another to mix their contents, deliver new patches of lipids to the membrane, and export waste and is a requisite of sexual reproduction. Membrane fusion is also required for the asexual delivery of genetic material through either viral or liposomal vehicles. It is clear that fusion is facilitated by, for example, SNARE (soluble *N*-ethylmaleimide fusion protein attachment protein receptor) and viral fusion proteins,[1a,b] but nonetheless understanding the dynamics of phospholipid bilayer transformation continues to be integral to developing a rational molecular picture of the events involved. Thus, there has been a great deal of focus on the interaction kinetics and thermodynamics of pure lipid systems. The development of experimental[2a] and theoretical[2b] methods to envisage the molecular dynamics of lipid bilayer fusion has been indispensable. An elegant fluorescence-based technique, introduced by Lentz and co-workers,[3a,b] was used to follow the progress of the poly(ethylene glycol) (PEG)-induced fusion of large and small unilamellar vesicles of phosphatidylserine (LUVs and SUVs, respectively). Their work provided significant evidence to support the hypothesis that membrane fusion dynamics involves a three-step process: aggregation, stalk formation, and mixing of vesicle contents. Recently, Yang and Huang confirmed the presence of stalks using X-ray diffraction to examine increasingly dehydrated multibilayers.[4] The next phase in understanding membrane fusion may come from examining structure and dynamics simultaneously. To that end, we are developing an LUV-based system where vesicle aggregation/fusion is monitored using two-photon excitation fluorescence cross-correlation spectroscopy (TPE-XCS).

TPE-XCS uses a type of fluctuation analysis that selectively examines the making and breaking of linkages between species bearing different fluorescent labels. TPE-XCS provides information about the concentrations of linked and unlinked species and their hydrodynamic sizes.[5] TPE-XCS measures fluorescence that is separated by wavelength and then collected simultaneously in two detection channels. The time-dependent instantaneous fluorescence intensity from each channel is then cross correlated in steps of time, τ. The time dependence (decay) of the XCS signal indicates the loss of the complex from the excitation volume, either by diffusion or dissociation. Thus, all stages of liposomal association/fusion can be easily measured because singly labeled liposomes average to zero in the generation of the cross-correlation function. An analysis of the XCS decay returns a diffusion coefficient for the fused species. Thus, the hydrodynamic size of the fused entity can be estimated using the Stokes−Einstein relationship.

Details of vesicle size change during fusion are important in understanding the process. Traditionally, vesicles have either been imaged using cryoelectron microscopy or sized using light-scattering methods. Although powerful, these methods have some drawbacks. For example, electron microscopy (EM) requires a huge number of vesicles to determine average sizes and can be time-consuming. Additionally, it would be difficult to collect simultaneous kinetic data on a single sample. Light scattering (dynamic and static) provides an alternative to EM, but the deconvolution of dynamic light scattering data to yield concentrations of species is challenging. The advantage of following vesicle size and concentration changes is that the order of fusion kinetics need no longer be inferred but rather is measured directly. In principle, by following the fused vesicle size distribution during the entire course of the process, the propensity toward the nucleation of vesicles or a limiting size of fused vesicles can be investigated.

To provide proof of the principle for the application of TPE-XCS to membrane fusion, we have chosen to investigate the novel system of dioleoyl phosphatidylcholine (DOPC)/halothane. Halothane, $CF_3CHClBr$, is a general anesthetic that readily partitions into lipid bilayers.[6] We and others[7] have shown that halothane incorporates into a bilayer just below the headgroup region and does so heterogeneously. This leads to greater area per lipid, greater flexibility, and possibly a reduction

* Corresponding author. E-mail: dcramb@mail.ucalgary.ca.
[†] University of Calgary.
[‡] University of Regina.

10.1021/jp037613t CCC: $27.50
Published on Web 06/22/2004

in void space as intervesicle stalks form during fusion. To our knowledge, there is no prior report of fusion induced solely by the incorporation of small, hydrophobic molecules into bilayers. The closest approach to the present one uses semifluorinated 10-carbon alkanes to moderate the Ca^{2+}-induced fusion of phosphatidylserine vesicles.[8] It is possible that halothane modifies the propensity toward fusion but does not affect the collision cross section for aggregation.

In the present study, we employed TPE-XCS as well as fluorescence dequenching and fluorescence brightness analysis to help decipher the mechanism of halothane-induced vesicle fusion. We have found that fusion proceeds initially via a dimerization mechanism and that the process reaches an equilibrium state. Under the conditions used, the process saturates at approximately six fused vesicles. This may indicate that halothane induces the hemifusion of DOPC LUVs.

Experimental Procedures

Stock solutions of DOPC (3.18×10^{-3} M), lissamine (red)-labeled dioleoylphosphatidyl-ethanolamine (DOPE) (7.86×10^{-5} M), and Oregon green (green)-labeled dipalmitoylphosphatidyl-ethanolamine (DPPE) (9.206×10^{-5}), suspended in methanol, were stored at −4 °C until needed. For the lissamine−DOPE-labeled DOPC vesicles, 314 μL of DOPC in methanol was pipetted into a 10-mL volumetric flask, and 25 μL of lissamine was added to the DOPC and then dried using N_2 gas until all solvent was removed. The sample was resuspended in PBS containing 320 mM sucrose. The Oregon green sample was prepared using 314 μL of DOPC in methanol and 8.6 μL of labeled Oregon green; it was then dried and resuspended in PBS containing 320 mM sucrose. Thus, we have a label/lipid mol ratio of $\sim 1/500$ for lissamine and $1/1300$ for Oregon green. It was necessary to use a larger initial ratio for lissamine because more of it is lost during extrusion. Both samples were stirred for 30 min at room temperature and protected from light. Following adequate mixing, the samples were alternately sonicated and stirred (four 10-min cycles). Sonication was achieved using a Bransonic 12 ultrasonic cleaner at 40 °C. After four cycles, the solutions were again stirred for 30 min and then transferred from the volumetric flask to scintillation vials for storage. Solutions were stored at 2 °C until use, and for the experiments reported, this was a period of no more than 3 days. Prior to experimentation, the solutions were extruded using an Avanti Polarlipids Inc. Miniextruder with a 100-nm nuclepore track-etch membrane obtained from Whatman nuclepore. Eleven passes through the extrusion device were sufficient to obtain uniform LUVs. This protocol was followed for all experiments.

For the fusion TPE-XCS experiment, equal-volume samples containing red DOPC LUVs and green DOPC LUVs were mixed by adding an aliquot (100 μL) of each of the red and green samples to a small scintillation vial and gently swirling. For halothane-containing samples, halothane (4 μL) was added to the vial, and the vial was gently swirled for 10 s, ensuring halothane saturation. (The saturation concentration of halothane in water is 17 mM.) This results in a final halothane-to-lipid mol ratio of 10.[6b] For kinetics experiments, the definition of time zero is when the swirling is complete. The samples were immediately placed in the sample chamber and placed on the inverted microscope. Some experiments were carried out by placing the samples on well slides and sealing them using Cytoseal. This process requires a drying time of 30 min, so the first spectrum was obtained 30 min after mixing. An open eight-chambered coverglass (NUNC) was used to measure the kinetics within the first 30 min after mixing.

Samples were excited using 780-nm, 100-fs laser light from a Spectra Physics Tsunami laser operating at 82 MHz. The laser power was attenuated to 20 mW with a neutral density filter to avoid photobleaching. Both Oregon green and lissamine have a reasonable two-photon excitation probability at 780 nm. The laser beam was expanded using a Galilean telescope to overfill slightly the back aperture of a 40×, 0.9-NA-long working distance Zeiss objective lens mounted on a Zeiss Axiovert 200. TPE fluorescence was collected by the same objective lens, passed through a broad bandpass filter to remove laser light (Omega Optical, XF3100), and reflected off of a dichroic optic (Chroma, 700DCSPXR) and through a tube lens in the side port of the microscope. The fluorescence then encounters a second dichroic optic (Chroma 565DCLP) to separate the red and green light. The spectrally separated light passes through bandpass filters (Chroma, E590LPv2 and D535/50× for the red and green emissions, respectively) and is coupled to optical fibers located at the focus of the tube lens. Using the optical fibers, we detected the fluorescence with two Si avalanche photodiodes (APDs, Perkin-Elmer, SPCQ-200). The output of the APDs is analyzed using a correlator card (ALV-5000, Langen, Germany) installed in a PC.

The size of the excitation volume was calibrated using a 125 nM aqueous solution of rhodamine 6G, whose diffusion coefficient is known (2.8×10^{-12} m^2/s),[5] as described in the Theory/Data Reduction section.

For the BODIPY (β-BODIPY-C5-HPC (530/550), Molecular Probes) dequenching lipid mixing assay, the LUVs were again prepared using the dry method. The final concentrations of the lipid after extrusion were as close as possible to that for the TPE-XCS study, given that lipid losses due to extrusion are not always exactly the same. The probe-to-DOPC ratio was 2 mol % for this assay. Subsequently, 5.0 mL of the unlabeled sample was added to 1.0 mL of the labeled sample and mixed gently. This solution (2.5 mL) was pipetted into a fluorescence cuvette, and an emission spectrum was collected. Halothane (2% v/v) was added to the solution, and the sample was inverted to ensure adequate and rapid mixing.[6] This results in a final halothane-to-lipid mol ratio of 10.[6] Fluorescence measurements were performed using a Varian Cary Eclipse with Eclipse software. A medium scan speed was chosen, and the slit widths were set to 5 nm. Emission spectra were collected by exciting the sample at 480 nm and collecting the emission from 490 to 700 nm. Scans were collected every 5 min for the first 30 min, followed by collection every 15 min after that for 300 min.

For the ANTS/DPX contents mixing assay,[9] the LUVs were also prepared using the dry method as stated in the above paragraph. However, for this assay LUVs were extruded in the presence of either 2.5 mM ANTS (8-aminonaphthalene-1,3,6-trisulfonic acid, Molecular Probes) or 25 mM DPX (*p*-xylene-bis-pyridinium bromide, Molecular Probes) in 10 mM TRIS−HCl buffer at pH 7.4. The extruded LUV solutions were dialyzed using Spectra/Por(R) Float-a-Lyzer (R) (MWCO of 1000 Da, Spectrum Laboratories, Inc), for 48 h. Approximately 1 mL of each LUV solution was combined in a fluorescence cuvette and mixed gently, and fluorescence spectra were recorded to ensure the LUVs' stability before adding halothane. Halothane (2% v/v) was added to the solution, and the sample was inverted to ensure adequate and rapid mixing as above. Emission spectra were collected by exciting the sample at 360 nm and collecting the emission from 370 to 700 nm. Scans were collected every 5 min for the first 15 min, followed by every 15 min after that for 60 min.

The collected spectra were plotted using Origin Pro 7.0. To determine the contribution for the β-BODIPY monomer and dimer peaks, the plots were changed to wavenumbers, and the spectra were fit using the sum of two Gaussian functions. The dimer peak was centered at 16 833 cm^{-1} (594 nm); the peak for the β-BODIPY monomer emission was centered at 17 953 cm^{-1} (557 nm). Holding these values constant, we could determine the ratios of the peak heights for each spectrum. The peak widths were found not to vary significantly. There was no spectral evidence of any solvatochromic effects of halothane on the BODIPY chromophore.

We confirmed that dequenching is due to a dilution of BODIPY concentration within the liposome bilayer by examining a series of probe concentrations over the range of 0.5−2.5 mol %. The decrease in the ratio of monomer-to-dimer peak height was found to vary with increasing probe concentration in a linear fashion.

Theory/Data Reduction. Autocorrelation decays were modeled assuming a Gaussian TPE volume using the equation

$$G(\tau) = \frac{\left(1 + \frac{8D\tau}{r_0^2}\right)^{-1}\left(1 + \frac{8D\tau}{z_0^2}\right)^{-1/2}}{\langle C\rangle\left(\frac{\pi}{2}\right)^{3/2} r_0^2 z_0} \quad (1)$$

where τ is the lagtime, D is the diffusion constant, C is the concentration of the diffusing species, r_0 is the laser beam radius (3.3×10^{-7} m) at its focus, and z_0 is the depth of focus (4.5×10^{-6} m). The TPE excitation volume was calibrated by measuring the ACF for a 100 nM solution of rhodamine 6G ($D = 2.8 \times 10^{-10}$ m^2/s) in pure H_2O. The excitation volume was found to be 2.5 fL ($\pi^{3/2} r_0^2 z_0$).

Cross-correlation decays were modeled as above using the equation

$$G_{ij}(\tau) = \frac{\langle C_{ij}\rangle\left(1 + \frac{8D_{ij}\tau}{r_0^2}\right)^{-1}\left(1 + \frac{8D_{ij}\tau}{z_0^2}\right)^{-1/2}}{\langle C_{ij} + C_i\rangle\langle C_{ij} + C_j\rangle\left(\frac{\pi}{2}\right)^{3/2} r_0^2 z_0} \quad (2)$$

where the subscripts i, j, and ij represent red-labeled, green-labeled, and dual-color-labeled diffusing species, respectively. Nonlinear least-squares fitting to the data was accomplished using the software package Origin.

Results and Discussion

In Figure 1, we show examples of two fluorescence histograms for a mixture of DOPC liposomes, half labeled with lissamine and half labeled with Oregon green. The spikes in fluorescence intensity represent individual LUVs traversing the excitation volume. From the larger red fluorescence signal, it appears that more lissamine remains incorporated in the vesicles after extrusion. Also, the avalanche photodiode detectors (APDs) have a higher quantum efficiency in the red than in the green. An inspection of the top panel suggests very little evidence of simultaneous events in the red and the green detection channels, representing a lack of fusion in the absence of a fusion-enhancing agent. The bottom panel reveals many coincident red and green events, signifying that dual-labeled species are passing through the excitation volume. Halothane, a general anesthetic, has been used as the fusion agent. Previously, we showed that halothane also acts as a fluorescence quencher when introduced to Laurdan labeled DOPC vesicles.[6a,b] The bottom panel of Figure 2 also reveals this behavior. The average fluorescence count rate in both channels is lower in the presence of halothane, which partitions just below the headgroups in a DOPC bilayer.[6b,7] Note that there is approximately 300 Hz of laser scatter noise in each channel and that the fluctuations in the green channel are built on top of this. These histograms are analyzed by cross correlation "on the fly" using hardware,[5] the results of which are displayed in Figure 2 for the halothane-containing sample.

It is apparent from Figure 2 that the cross-correlation functions, $G_x(\tau)$, level off as τ approaches 0 and decay between approximately 10 and 500 ms. The flat portion at early lag time is proportional to the number of dual-labeled (i.e., fused) vesicles in the sample, and the decay time reflects the diffusion dynamics required for the vesicle to exit the excitation volume. This Figure also shows that as the time of mixing increases the flat portion (a.k.a. $G_x(0)$) also increases in accordance with an increase in the concentration of fused vesicles. The change in the decay time is less obvious. We can compare these results with control experiments, where the vesicles are mixed in the absence of halothane (Figure 3b). In the absence of halothane, essentially no fusion takes place. The small TPE-XCS signal observed in Figure 3b is due to a limited amount of cross talk between the detection channels and is accounted for in the analysis of the cross-correlation decay according to the method of Schwille and co-workers.[5] In fact, the vesicle solution in the absence of halothane was observed to be stable over a period of 3 days (Supporting Information).

One can model the TPE cross-correlation function assuming a 3-D Gaussian-shaped excitation volume using the method developed by Schwille and co-workers.[5] The cross-correlation decays were fit to eq 2 to determine changes in the concentrations and diffusion coefficients of the aggregated/fused species as fusion progressed. The results of the fits are tabulated in Table 1 (Supporting Information). An example of the data and fit is presented in Figure 3. The resulting concentrations of fused species and their diffusion coefficients are plotted in Figure 4a as a function of time following mixing. Assuming a simple binary reaction for the aggregation−fusion process measured here, we can model the kinetics of increased vesicle fusion using the second-order integrated rate law (represented by the red line in Figure 4a). It is notable in Figure 4b that the diffusion coefficient of the fused species fluctuates more significantly than the number of fused vesicles. This is likely due to the fact that a distribution of sizes is present in the sample once fusion begins. The halothane-induced aggregation/fusion constant of 4.9×10^3 M^{-1} s^{-1} is considerably smaller than that for Ca^{2+}-induced DOPC/cardiolipin LUVs, 3.5×10^6 M^{-1} s^{-1}.[3a] Thus, it appears that the concentration of halothane used does not lower the fusion activation barrier to the same degree as cardiolipin.

The diffusion coefficients of fused vesicles are in the range of $(6.5-2.0) \times 10^{-13}$ m^2/s, putting the hydrodynamic Stokes−Einstein radius (assuming to be a spherical diffuser) at ~200 nm. This is 1.5−3.3 times the radius we measure for DOPC LUVs in the absence of halothane, suggesting that the aggregates initially resemble two LUVs. It was previously shown[10a,b] that aggregation is the rate-limiting step in the membrane fusion process, and thus we assume that the aggregates form, fuse, and mix lipids/contents. XCS is more sensitive to aggregation than alternate techniques because it is not necessary to mix the labels to detect an XCS signal. If one takes the vesicle surface area of six spheres and combines them to produce one larger sphere, then the radius should increase by $\sqrt{6}$ or 2.5. We find

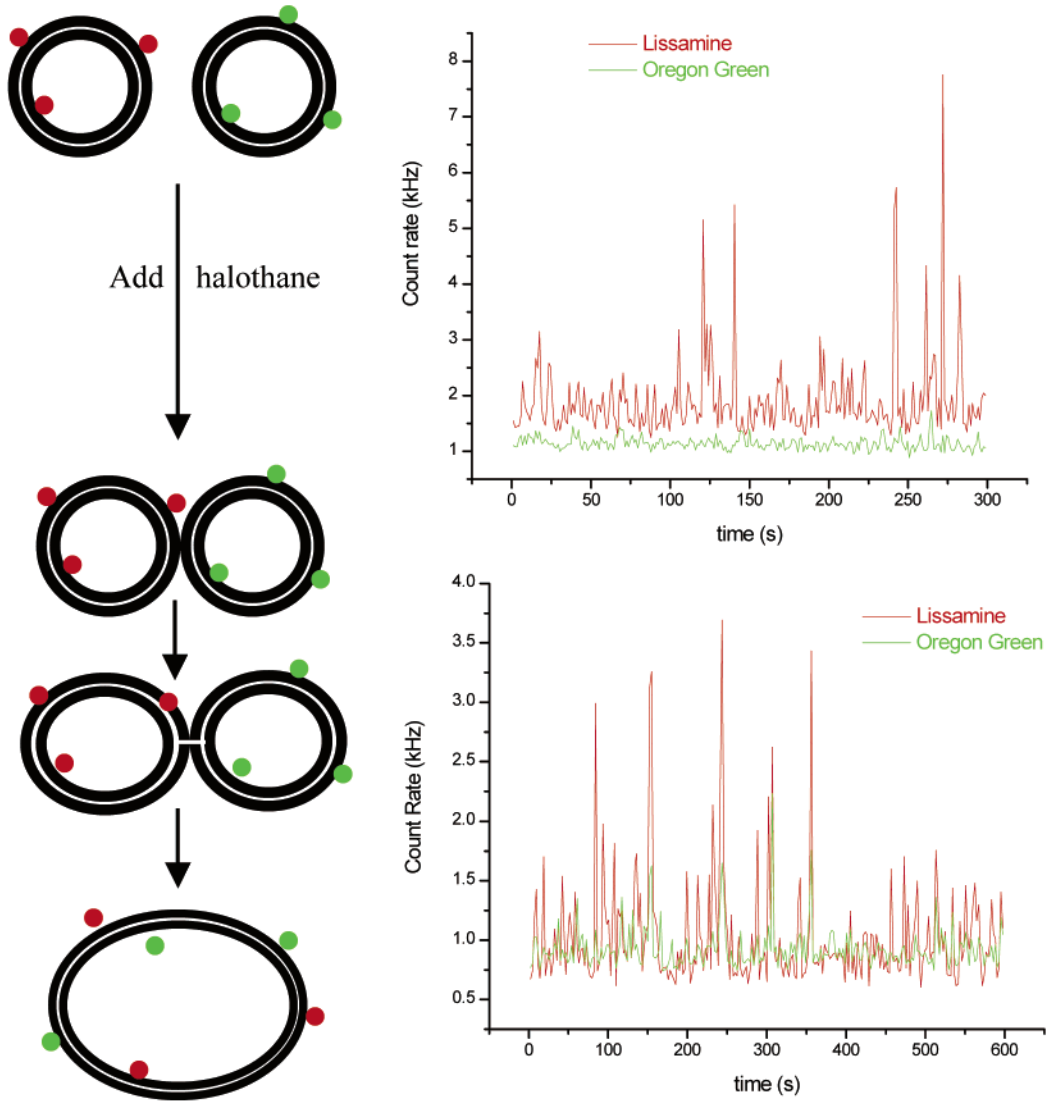

Figure 1. Schematic and fluorescence histograms for mixtures of DOPC liposomes labeled with lissamine−DOPE (red) and Oregon green−DPPC (green) dyes. The upper panel shows a typical histogram for a mixture without halothane. The lower panel shows a histogram typical of the mixture with halothane. The left side of the lower panel indicates the structures of associated vesicles that would result in a dual-labeled vesicle.

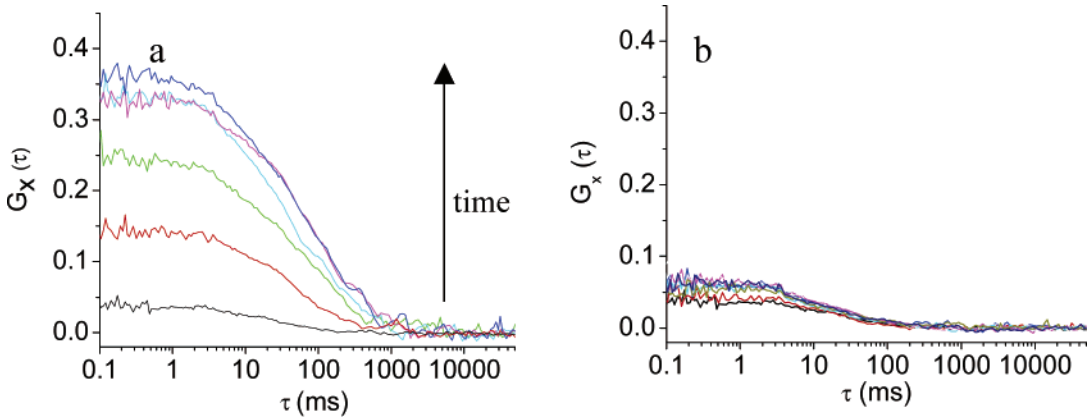

Figure 2. Cross-correlation functions of a mixture of red- and green-labeled DOPC vesicles as a function of time of mixing. (a) With halothane added, $G_x(0)$ values increase with time and then asymptotically approach 0.35. The decay times do not appear to vary significantly. (b) Without halothane, there is a slight increase in $G_x(0)$.

an increase of 3.3, which may reflect that the shape of the larger fused vesicles is no longer spherical. If the larger vesicles were oblate, then this increase in the diffusion constant could result from an ellipsoid with dimensions of 140 nm × 85 nm.[11]

To answer the question of whether we are observing fusion or hemifusion, we attempted to examine the brightness of the fluorescence labels as a function of time.[12] This is challenging for our system because the fluorescence histograms necessarily

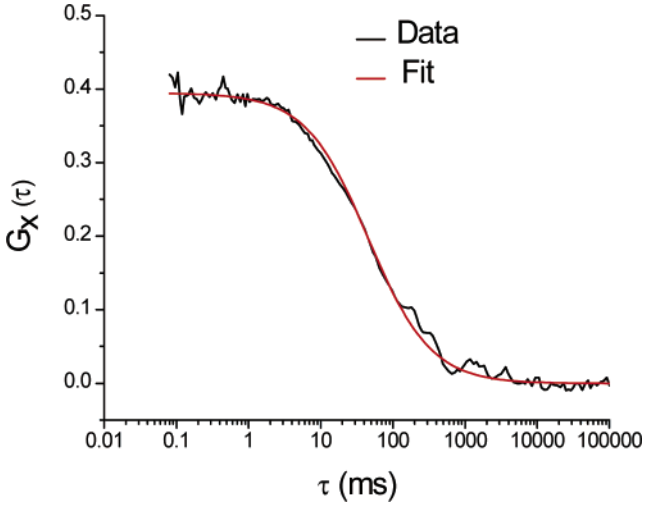

Figure 3. Cross-correlation decay (black) and fit (red). The fit was obtained using eq 2 for a mixture of red- and green-labeled DOPC vesicles in the presence of halothane.

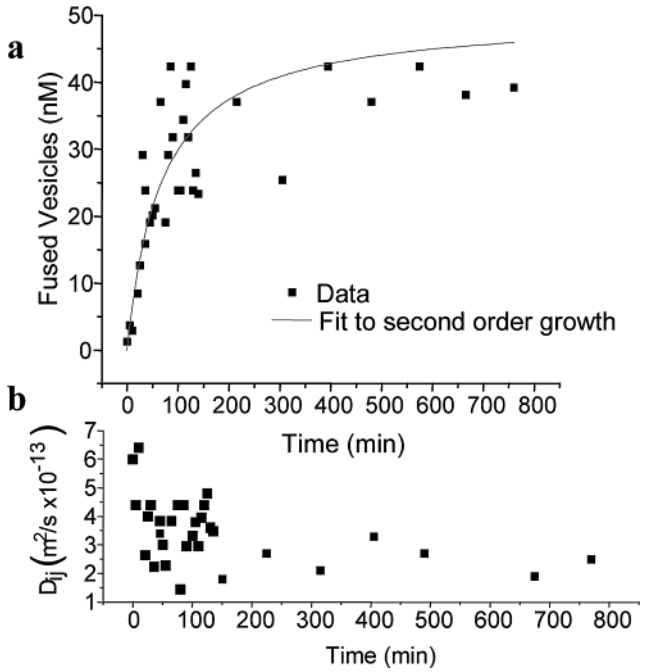

Figure 4. Data resulting from fits of cross-correlation decays as a function of time after mixing vesicles in the presence of halothane. (a) Increase in the concentration of fused halothane-containing DOPC vesicles and (b) diffusion coefficients of fused vesicles versus time.

undergo a change in brightness during fusion. That is, pairs of like-colored diffusing species that have associated will be twice as bright as at time zero. This, coupled with the distribution of fluorescent tags within a given vesicle, meant that a statistical analysis of the brightness change of Oregon green and lissamine as an indication of fusion was inconclusive. However, when we used a variation of the method of using the loss of BODIPY fluorescence energy transfer (FRET)[13] as an indicator, compelling evidence for lipid mixing promoted by halothane was observed. We were able to follow the loss of a BODIPY-C5-HPC (530/550) dimer peak as a function of time. The only mechanism for this change is the dilution of the probe in the lipid environment brought on by the fusion or hemifusion of vesicles. The data are plotted in Figure 5. In the absence of halothane, no change in the ratio of the peaks in Figure 5 was observed. In the presence of halothane, the kinetics of monomer/dimer fluorescence peaks is exactly the same as that observed using TPE-XCS. However, with TPE-XCS we are able to follow simultaneously the increase in (hemi)fused species and their diffusion constants. Within experimental uncertainty, the kinetic data derived from dequenching and from TPE-XCS overlap completely. The dequenching data have less scatter because dequenching is sensitive only to a change in the lipid/probe ratio. The scatter in the TPE-XCS-derived data results from the heterogeneity of fused particle sizes during the middle stages of fusion. Moreover, it is not trivial to extract absolute concentrations of fused vesicles from these data, and the dequenching data do not contain information about the sizes and size distribution of (hemi)fused vesicles.

In the literature, fusion and hemifusion are distinguished as the difference between intervesicle contents mixing and intervesicle lipid mixing. The above assay provides evidence of the latter but not the former. Therefore, a fluorescence quenching assay was performed in which half of the LUVs were loaded with ANTS and half were loaded with DPX. Upon contents mixing, DPX will quench the fluorescence of ANTS.[9] Thus, ANTS- and DPX-loaded LUVs were mixed together, and halothane was administered. Conditions were chosen to mimic closely those used in the XCS experiments. Aggregation was confirmed under these conditions through an increase in light scattering and by using FCS to follow the increasing vesicle size. Also observed was a 45% decrease in fluorescence intensity due to contents mixing (Figure 6). In the absence of halothane, no contents mixing was observed. This evidence coupled with the previous results is very suggestive that halothane induces the association of DOPC LUVs and a significant fusion of these aggregates.

For other fluorescence and light-scattering techniques, detecting the earliest stages of aggregation is a significant challenge. It is clear from Figure 1 that by observing simultaneous events in both channels of the fluorescence histogram one immediately knows that aggregation/fusion is taking place. Moreover, the sensitivity of TPE-XCS allows the absolute minimum of the fluorescence label to be used. Thus, the possibility of label-induced artifacts in the measured kinetics and structure is minimized. The size measured for the fused particles gives us confidence in modeling the aggregation kinetics as an association reaction, initially second order in vesicle concentration. Clearly, as the time of reaction progresses, larger, more complex aggregates may form,[10b] which may reflect the systematic deviation of the fit from the data at longer time. The decrease in the diffusion coefficient (i.e., the increase in the size of fused particles) at longer time may reflect higher-order fusion events (such as one fused vesicle aggregating with an LUV) creeping into the process. In the absence of halothane, no fusion takes place (data not shown).

It is interesting to speculate on the mechanism by which halothane enhances aggregation and fusion. We have previously shown using fluorescence quenching and atomic force microscopy[6a,b] that halothane localizes just beneath the headgroups of DOPC in a bilayer and does so in a cooperative fashion. The result is that local halothane-rich domains form that are thinner and less rigid because halothane increases the interlipid spacing. It is plausible that this would increase the propensity both for the aggregation and fusion of DOPC vesicles. With increased lipid spacing, random collisions between vesicles become less elastic because lipid headgroups from each vesicle may interpenetrate, leading to aggregation. Then the void-filling propensity of halothane may lower the energy of stalk formation during fusion. From Figure 5, it appears that fusion immediately follows

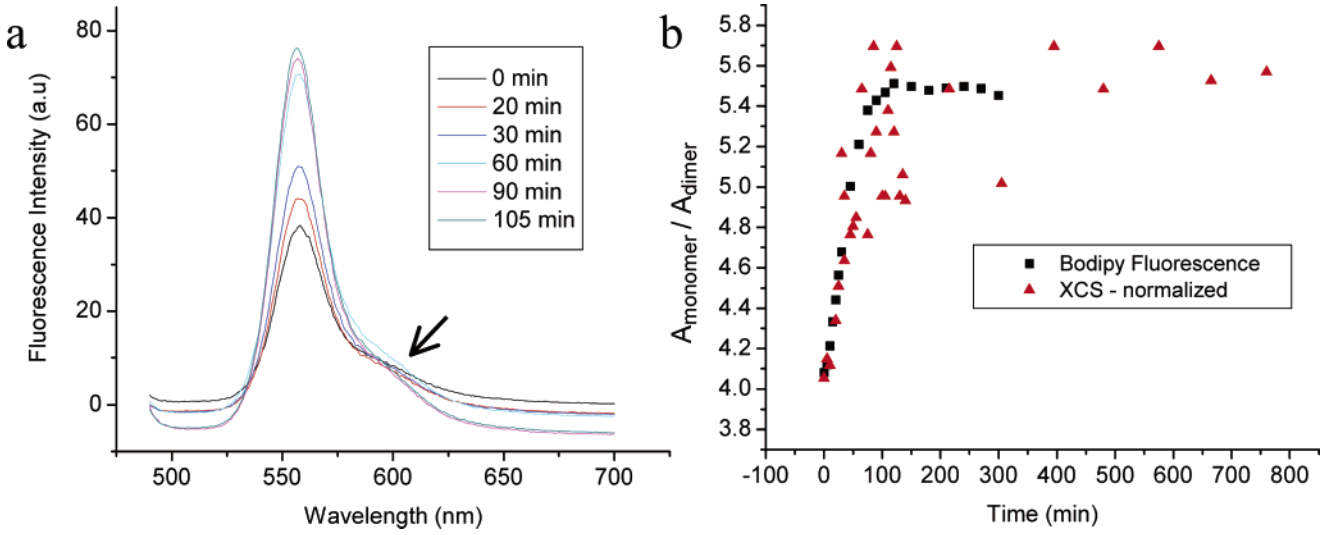

Figure 5. BODIPY-C5-HPC (530/550) dequenching assay for vesicle fusion. (a) Fluorescence spectra of BODIPY-550-labeled DOPC vesicles in a solution of unlabeled DOPC vesicles as a function of time after halothane addition. Note the increase in monomer fluorescence as the labeled and unlabeled vesicles undergo fusion. The arrow indicates the position of the dimer peak. (b) Plot of the ratio of the deconvoluted contributions of monomer and dimer peaks in part a as a function of time after halothane addition. See the text for more experimental and deconvolution details. Also included are the data from Figure 3a normalized to dequenching data.

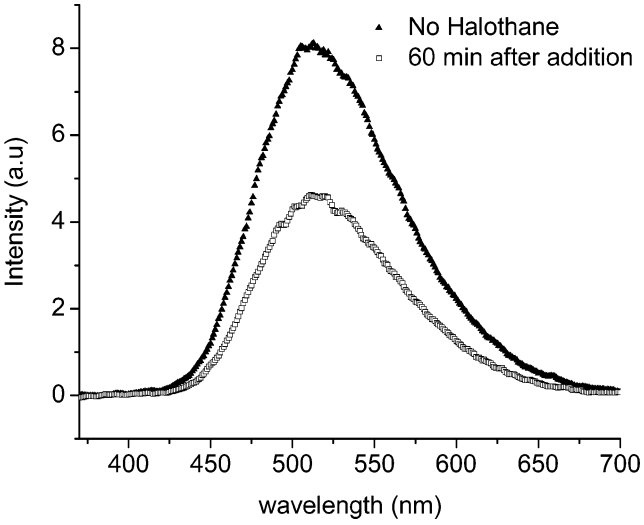

Figure 6. Spectra of DOPC LUVs loaded with ANTS in the presence of DOPC LUVs loaded with DPX (quencher). Upon the addition of halothane 2% v/v, significant quenching of ANTS by DPX is observed, indicating contents mixing between fused LUVs. ANTS was excited at 360 nm.

aggregation because the kinetics of aggregation and fusion are the same within experimental uncertainty.

Conclusions

We have demonstrated, using two-photon fluorescence cross-correlation spectroscopy (TPE-XCS), that in the presence of halothane appreciable fusion between DOPC vesicles takes place. TPE-XCS provides a new look at the fusion process because changes in both vesicle concentration and size can be monitored simultaneously. Thus, it was possible to observe directly the emerging heterogeneity of a solution of vesicles undergoing fusion. Additionally, the novel fusion agent, halothane, likely induces fusion by lowering the energy barrier to stalk formation, where void spaces and high curvature in and around the lipid stalk are thought to be the major factors that limit the rate of fusion. We and others have shown that halothane incorporates into a bilayer just below the headgroup region and does so heterogeneously. This leads to a greater area per lipid, greater flexibility, and possibly a reduction in void space as intervesicle stalks form during fusion. We have revealed that this fusion agent is very gentle, allowing the earliest stages in fusion to be examined solely by altering the bilayer environment.

Acknowledgment. This work is supported by the Natural Sciences and Research Council of Canada and by AstraZeneca. J.L.S. is grateful to the Alberta Ingenuity Fund for support in the form of a scholarship. We thank Professor Elmar Prenner (University of Calgary) for his insightful comments and help with the fusion assay.

Supporting Information Available: Diffusion coefficients. Autocorrelation decays of DOPC SUVs labeled with lissamine−DOPE in the absence of halothane. This material is available free of charge via the Internet at http://pubs.acs.org.

References and Notes

(1) (a) Nickel, W.; Weber, T.; McNew, J. A.; Parlatti, F.; Söllner, T. H.; Rothman, J. E. *Proc. Natl. Acad. Sci. U.S.A.* **1999**, *96*, 12571−12576 (b) Jahn, R.; Grubmüller, H. *Curr. Opin. Cell Biol.* **2002**, *14*, 488−495.

(2) (a) Hu, K.; Carroll, J.; Gedorovich, S.; Rickman, C.; Sukhodub, A.; Davletov, B. *Nature* **2002**, *415*, 646−650 (b) Kozlovsky, Pl.; Kozlov, M. M. *Biophys. J.* **2002**, *82*, 882−895.

(3) (a) Lentz, B. R.; Lee, J. K. *Mol. Membr. Biol.* **1999**, *16*, 279−296. (b) Haque, Md. E.; McIntosh, T. J.; Lentz, B. R. *Biochemistry* **2001**, *40*, 4340−4348.

(4) Yang, L.; Huang, H. W. *Science* **2002**, *297*, 1877−1879.

(5) Heinze, K. G.; Koltermann, A.; Schwille, P. *Proc. Nat. Acad. Sci U.S.A.* **2000**, *97*, 10377−10382.

(6) (a) Leonenko, Z. V.; Cramb, D. T. *Can J. Chem.*, in press, 2004. (b) Carnini, A.; Phillips, H. A.; Shamrakov, L. G.; Cramb, D. T. *Can. J. Chem.*, in press, 2004.

(7) Koubi, L.; Tarek, M.; Klein, M. L.; Scharf, D. *Biophys. J.* **2000**, *78*, 800−811.

(8) Ferro, Y.; Krafft, M. P. *Biochim. Biophys. Acta* **2002**, *1581*, 11−20.

(9) Ellens, H.; Bentz, J.; Szoka, F. C. *Biochemistry* **1985**, *24*, 3099−3106

(10) (a) Wilschut, J.; Nir, S.; Scholma, J.; Hoekstra, D. *Biochemistry* **1985**, 4630−4636. (b) Nir, S.; Bentz, J.; Wilschut, J. *Biochemistry* **1980**, *19*, 6030−6036.

(11) Berg, H. C. *Random Walks in Biology*; Princeton University Press: Princeton, NJ, 1993.

(12) Palo, K.; Brand, L.; Eggeling, C.; Jäger, S.; Kask, P.; Gall, K. *Biophys. J.* **2002**, *83*, 605−618.

(13) Malinin, V. S.; Haque, M. E.; Lentz, B. R. *Biochemistry* **2001**, *40*, 8292−8299.